

How to Cite:

Alhussien, M. A., & Abd, A. N. (2022). Synthesis and characterization of pure and Au doped Fe₃O₄ using co-precipitation method. *International Journal of Health Sciences*, 6(S4), 12537–12545. <https://doi.org/10.53730/ijhs.v6nS4.12058>

Synthesis and characterization of pure and Au doped Fe₃O₄ using co-precipitation method

Mohammed Abdul Alhussien

Chemistry department, college of science, Diyala university

Ahmed N. Abd

Chemistry department, college of science, Diyala university

Abstract---In this research, a sonochemical activation-assisted biosynthesis of Au/Fe₃O₄ nanoparticles is proposed. The proposed synthesis methodology incorporates the use of *Piper auritum* (an endemic plant) as reducing agent and in a complementary way, an ultrasonication process to promote the synthesis of the plasmonic/magnetic nanoparticles (Au/Fe₃O₄). The synergic effect of the green and sonochemical synthesis favors the well-dispersion of precursor salts and the subsequent growth of the Au/Fe₃O₄ nanoparticles. The hybrid green/sonochemical process generates an economical, ecological and simplified alternative to synthesizing Au/Fe₃O₄ nanoparticles with enhanced catalytic activity, pronounced magnetic properties. The morphological, chemical and structural characterization was carried out by high-resolution Scanning electron microscopy (HR-SEM), Energy Dispersive X-Ray Spectroscopy (EDS) and X-Ray diffraction (XRD), respectively. Ultraviolet-visible (UV-vis) and X-ray photoelectron (XPS) spectroscopy confirm the Au/Fe₃O₄ nanoparticles obtention. Finally, the catalytic activity was evaluated by sonocatalytic degradation of methyl orange (MO). In this stage, it was possible to achieve a removal percentage of 91.2% at 15 min of the sonocatalytic process (160 W/42 kHz). The initial concentration of the MO was 20 mg L⁻¹, and the Fe₃O₄-Au dosage was 0.075 g L⁻¹. The MO degradation process was described mathematically by four kinetic adsorption models: Pseudo-first order model, Pseudo-second order model, Elovich and intraparticle diffusion model.

Keywords---synthesis, characterization pure, Au doped Fe₃O₄, co-precipitation method.

Introduction

In recent years, the magnetic-plasmonic materials have been widely studied due to their applications as bifunctional nanomaterials in several areas, including biolobiomedicine, bio-labelling, optics, electronics and catalysis [1-2]. Generally, the magnetic-plasmonic materials are composed in their magnetic part by superparamagnetic iron oxides nanoparticles (SPION), which are employed in wastewater treatment, heterogeneous catalysis, drug delivery, cancer treatment, magnetic resonance imaging (MRI), biological separation, photocatalysis and hyperthermia [3-4]. Regarding the plasmonic part, are composed of a noble metal such as Au. In whose case has been employed in electrochemical sensors, biocompatible systems, as antibacterial material and advanced oxidation process (AOPs) [5-6]. Recently, the AOPs has reported a high efficiency in wastewater treatment and pollutant degradation due to the AOPs promote the formation of highly reactive hydroxyl radicals, which exhibits a significant oxidation potential [7- 9]. Some AOPs such as sonolysis, sonocatalysis, sonophotocatalysis, electro-Coagulation, electro-peroxene and Fenton process, among others, has been employed in the degradation of Methylene Blue, Methyl Orange, Acid Orange 7 (AO7), Basic Violet 10 (BV10), diclofenac, ciprofloxacin, moxifloxacin, Arsenate, Auramine-O (AO, acid blue 129, Chromium, nitrophenol [8,10-11]. Nonetheless, the properties of the magnetic-plasmonic materials depend in great measure of the morphology and particle size distribution [12]. In this sense, the implementation and study of new methodologies to synthesize magnetic plasmonic materials are focused on the green chemical and the use of the physico-chemical procedures that reduce or eliminate the use of toxic chemical reagents [13-15]. In recent years, sonochemistry has been widely studied due that offers a great quantity of application in many fields of knowledge. Nonetheless, the potential sonochemistry applications have not been exploited in deep [13,14]. Specifically, in the sonochemical synthesis of nanomaterials, the use of ultrasound in chemical reactions, favors the dispersion of the reactive species in the synthesis process. The propagation of ultrasound waves in a liquid generates the acoustic cavitation phenomena, which provide a mechanical activation to the reaction, given as result the destruction of the attractive forces of molecules in the liquid phase [1]. The sonochemical synthesis has been generally employed to obtain well-dispersed and core-shell type nanoparticles [1]. On the other hand, the employ of the green chemistry in the synthesis of metallic and bimetallic nanoparticles has covered a preponderant role due to the green chemistry reduce or eliminate the use and/or generation of hazardous substances [5,16,17]. In this sense, the great quantity of organic and biocompatible components presents in the plant extracts (antioxidants, phenolic compounds, flavonoids, also known as secondary metabolites, which including the flavones, flavanols, isoflavones, flavanones and anthocyanidins), have promoted the use of plant extracts as reducing or stabilizing agents in the synthesis of nanomaterials, due that these organic components are directly involved in the reduction of metallic ions of the precursors [18,19]. The use of the endemic plant species such as *Cynara cardunculus*, *Silybum marianum*, *Lonicera japonica*, *Melissa officinalis*, *Artemisia absinthium*, *Anthemis nobilis*, *Lonicera japonica*, *Thymus kotschyanus*, *Moringa oleifera* flower, *Cnicus Benedictus* and *Justicia spicigera* were reported in the obtention of Au and Fe₃O₄ NP's [20-21]. Nonetheless, the *Piper auritum* extract, has not been employed for the magnetic plasmonic nanoparticles of Au/Fe₃O₄

composition. The *Piper auritum* is an endemic and medicinal plant that grows in the tropical area of Central America. The *Piper auritum*, offers antimicrobial properties due to the great quantity of phytoalexins in their composition, which are compound of low molecular weight in the *Piper auritum* as result of the biotic and abiotic stresses [22-23]. In this sense, this work proposes the green synthesis of Au/Fe₃O₄ nanoparticles by *Piper auritum* extract and sonochemical activation. The synergic effect of the green synthesis and the sonochemical synthesis offers a functional methodology to the obtention of Au/Fe₃O₄ nanoparticles with significant catalytic and magnetic properties. Complementary, the sonocatalytic degradation of methyl orange is also studied, being possible to achieve a removal percentage of 91.2% at 15 min of the sonocatalytic process (160 W/42 kHz). Is important to mentioning that result obtained were highly competitive in relation to those reported in the literature, considering the simplification and economy of the catalyst synthesis route, as well as the low power of the ultrasound equipment and mainly the short period of time in which the sonocatalytic degradation was carried out.

Experimental

Materials

All source chemicals were supplied from Sigma-Aldrich company and used without any future purification.

Synthesis of Au/Fe₃O₄ nanoparticles

1 and 2 mM HAuCl₄.3H₂O were mixed separately with 0.1g ferric oxide in two 100ml beakers. Then 3ml of 1M sodium citrate solution was added, and the temperature was raised to 80°C until the solution turned purple. It was then filtered and rinsed in 50ml of ethanol, acetone, and distilled water and dried for three hours at 70°C.

Synthesis of Fe₃O₄ nanoparticles

In a separate 250ml glass beaker, 1g of Iron nitrate ninehydrate Fe(NO₃)₃.9H₂O was mixed with 50 ml deionized water to make Fe₃O₄ NPs. After 2 hours, add drops by drops of the NH₄OH solution contained in the mentioned solution to obtain a dark brown precipitate. To obtain nanoparticles, the powder was calcined at 400 C for 4 hours after being kept in the oven for 24 hours.

Results and Discussion.

Scanning electron microscopy (SEM)

Fig. 1(A) shows the scanning electron microscopy of Ferric oxide Fe₃O₄ with magnification strength 200 nm and 500 nm, respectively. It seems that the Ferric oxide is irregular in shape, and the particle size is in the range (40nm – 59nm). The surface of nanoparticles is porous and contains pores and bumps, as well as particle distribution is heterogeneous. Fig. 1(B) shows the scanning electron microscopy images of Au(0.8)/Fe₃O₄ nano oxide with a magnifying force of 200

nm and 500 nm, respectively. This explains that Au/Fe₃O₄ nano oxide was in form of irregularly shaped nanoparticles with various small and large grain sizes, and the particle size is in the range (26.86nm – 36.26nm). The Surface of Au(0.8)/Fe₃O₄ is porous and contains pores and rough. Fig. 1(C) show the scanning electron microscopy images of Au(1.6)/Fe₃O₄ nano oxide with a magnifying force of 200 nm and 500 nm, respectively. The image shows that the shape of the particles is heterogeneous and irregular as the surface of the particles contain pores and be bumpy. The particle size is between (29.11nm-49.01nm).

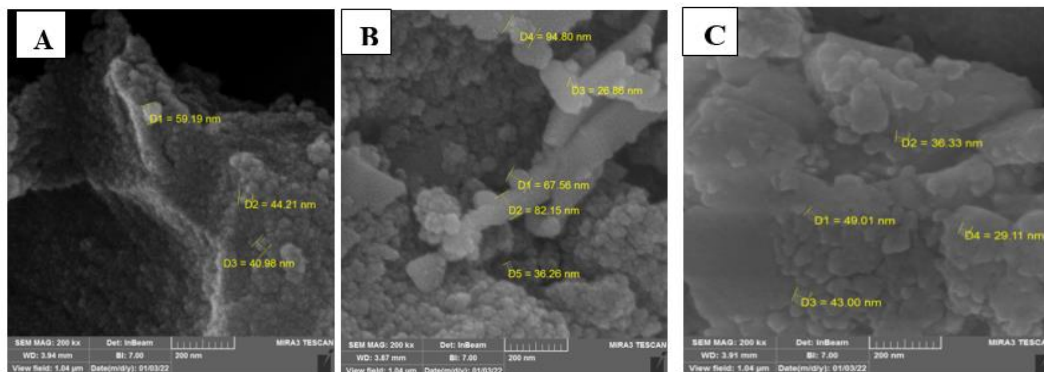


Fig 1: FESEM of (A) Fe₃O₄, (B) Au(0.8)-dopedFe₃O₄ and (C) Au(1.6)-dopedFe₃O₄

X-Ray diffraction analysis.

Fig. 1(A) shows. The XRD of sample in Table (1) shows the formation of Fe₃O₄ based on the comparison of their XRD patterns with the standard patterns of Fe₃O₄ (JCPDS 00-019-0629) of cubic phase structure. The diffraction peaks corresponding to (311), (533), (400), (440), (511), (220) and (111) are quite identical to characteristic peaks of the Fe₃O₄ crystal. The estimated particle size of the ferric nano oxide is (11.64nm). The presence of sharp peaks in XRD samples and particle size of less than (100) nm refers to the nanocrystalline nature of the surface. Fig. 1(B) shows . The XRD of sample in Table (2) shows the formation of Au(0.8Mm)/Fe₃O₄ based on the comparison of their XRD patterns with the standard patterns of Au/ Fe₃O₄, (Fe₃O₄ JCPDS 00-019-0629) (Au JCPDS 00-004-0784) of cubic phase structure. The diffraction peaks corresponding to (311), (400), (533), (511), (220) and (440) and doped Au to (111), (200) and (220) are quite identical to characteristic peaks of the Au/Fe₃O₄ crystal. The estimated particle size of the Au/Fe₃O₄ nano oxide is (17) nm. The presence of sharp peaks in XRD samples and particle size of less than (100) nm refers to the nanocrystalline nature of the surface.

Fig.1(C) The XRD of sample in Table (3) shows the formation of Au/Fe₃O₄ based on the comparison of their XRD patterns with the standard patterns of Au(0.1.6Mm)/ Fe₃O₄, (Fe₃O₄ JCPDS 00-019-0629) (Au JCPDS 00-004-0784) of cubic phase structure. The diffraction peaks corresponding to (311), (400), (533), (511), (422), (220), (111) and (440), doped (Au) to (111), (200) and (220) are quite identical to characteristic peaks of the Au/Fe₃O₄ crystal. The estimated particle size of the Au/Fe₃O₄ nano oxide is (21) nm. The presence of sharp peaks in XRD

samples and particle size of less than (100) nm refers to the nanocrystalline nature of the surface.

Table .2. XRD Parameter associated to the Au/Fe₃O₄ nanoparticles

hkl	2θ	d-spacing	FWHM	Size
Fe ₃ O ₄	35.6329	2.51757	0.7200	11.64
Au/Fe ₃ O ₄ (0.8mM)	35.098	2.5547	0.491	17
Au/Fe ₃ O ₄ (1.6mM)	35.305	2.5401	0.399	21

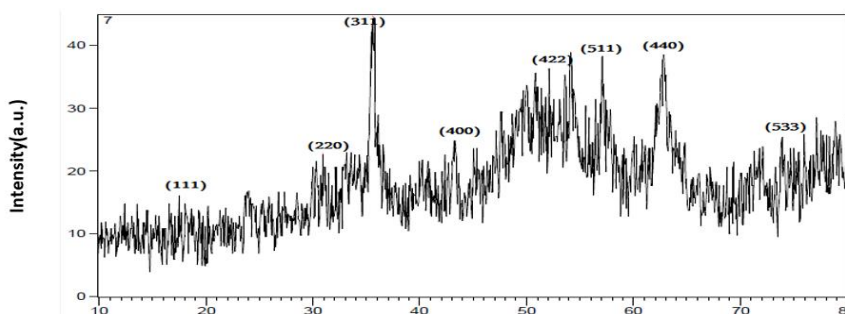


Fig.1(A) 2θ(Degree)

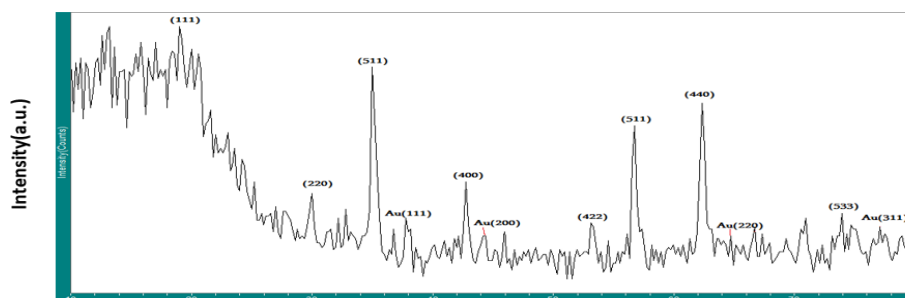


Fig.1(B) 2θ(Degree)

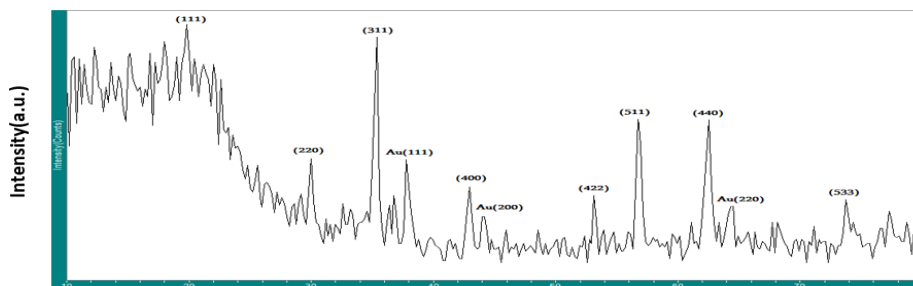


Fig.1(C) 2θ(Degree)

Fig 1: XRD of (A) Fe₃O₄, (B) Au(0.8)-dopedFe₃O₄ and (C) Au(1.6)-dopedFe₃O₄.

Energy Dispersive X-ray Analysis (EDXA)

The EDXA is used to represent the presence of elements and their percentage in nature. Figures (1, 2, and 3) show the EDXA result of CuO, Fe₃O₄, Au(0.8)-doped Fe₃O₄, Au(1.6)-doped Fe₃O₄, nanoparticles.

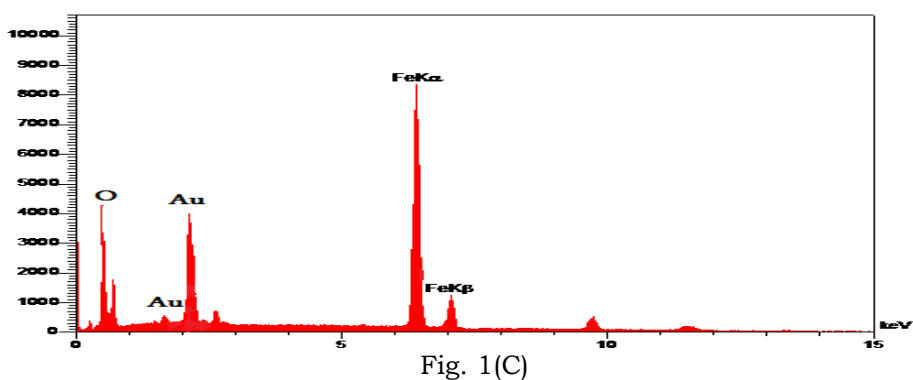
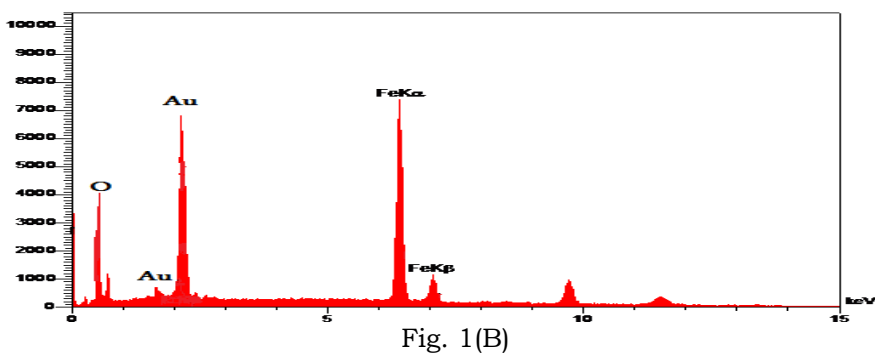
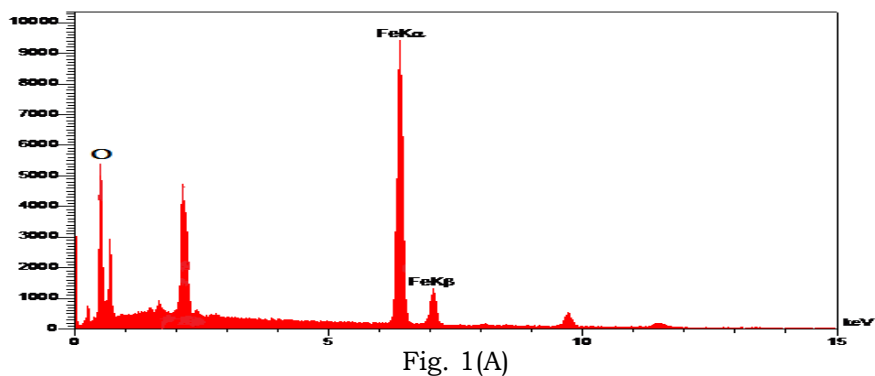


Fig 1: EDXA of (A) Fe₃O₄, (B) Au(0.8)-doped Fe₃O₄ and (C) Au(1.6)-doped Fe₃O₄.

Conclusion

In summary, the preparation of Au coated Fe₃O₄ nanoparticles by the co-precipitation method was reported in the present work and the structure,

functional groups, morphology and magnetization properties were examined using different techniques, the average crystallite and the physical size of the produced nanoparticles were found to decrease with increasing weight of Au. The prepared Au coated Fe₃O₄ nanoparticles exhibit superparamagnetic behavior and high saturation magnetization. Therefore the superparamagnetic and high saturation magnetization of Au coated Fe₃O₄ nanoparticles is promising biomedical applications such as MRI and biosensors.

References

1. Aguilar-Urquizo, E., Itza-Ortiz, M. F., Sangines-Garcia, J. R., Pineiro-Vázquez, A. T., Reyes-Ramirez, A., & Pinacho-Santana, B. (2020). Phytobiotic activity of piper auritum and ocimum basilicum on avian e. Coli. *Brazilian Journal of Poultry Science*, 22.
2. Bindes, M. M. M., Reis, M. H. M., Cardoso, V. L., & Boffito, D. C. (2019). Ultrasound-assisted extraction of bioactive compounds from green tea leaves and clarification with natural coagulants (chitosan and Moringa oleifera seeds). *Ultrasonics sonochemistry*, 51, pp. 111-119.
3. Conde-Hernández, L. A., & Guerrero-Beltrán, J. Á. (2014). Total phenolics and antioxidant activity of Piper auritum and Porophyllum ruderales. *Food chemistry*, 142, pp. 455-460.
4. Crase, S. J., Hockaday, C., & McCarville, P. C. (2007). Brief report: Perceptions of positive and negative support: Do they differ for pregnant/parenting adolescents and nonpregnant, nonparenting adolescents?. *Journal of Adolescence*, 30(3), pp. 505-512.
5. de Jesús Ruíz-Baltazar, Á. (2020). Green synthesis assisted by sonochemical activation of Fe₃O₄-Ag nano-alloys: Structural characterization and studies of sorption of cationic dyes. *Inorganic Chemistry Communications*, 120, p. 108148.
6. de Jesus Ruiz-Baltazar, A. (2020). Kinetic adsorption models of silver nanoparticles biosynthesized by Cnicus Benedictus: Study of the photocatalytic degradation of methylene blue and antibacterial activity. *Inorganic Chemistry Communications*, 120, p. 108158.
7. de Jesús Ruíz-Baltazar, Á., Reyes-López, S. Y., de Lourdes Mondragón-Sánchez, M., Estevez, M., Hernández-Martínez, A. R., & Pérez, R. (2018). Biosynthesis of Ag nanoparticles using Cynara cardunculus leaf extract: evaluation of their antibacterial and electrochemical activity. *Results in Physics*, 11, pp. 1142-1149.
8. Eghbali, P., Hassani, A., Sündü, B., & Metin, Ö. (2019). Strontium titanate nanocubes assembled on mesoporous graphitic carbon nitride (SrTiO₃/mpg-C₃N₄): Preparation, characterization and catalytic performance. *Journal of Molecular Liquids*, 290, p. 111208.
9. Elshikh, M. S., Chen, T. W., Mani, G., Chen, S. M., Huang, P. J., Ali, M. A., ... & Al-Mohaimed, A. M. (2021). Green sonochemical synthesis and fabrication of cubic MnFe₂O₄ electrocatalyst decorated carbon nitride nanohybrid for neurotransmitter detection in serum samples. *Ultrasonics sonochemistry*, 70, p. 105305.
10. Ghanbari, F., Zirrahi, F., Lin, K. Y. A., Kakavandi, B., & Hassani, A. (2020). Enhanced electro-peroxone using ultrasound irradiation for the degradation

- of organic compounds: A comparative study. *Journal of Environmental Chemical Engineering*, 8(5), p.104167.
11. Jain, B., Hashmi, A., Sanwaria, S., Singh, A. K., Susan, M. A. B. H., & Carabineiro, S. A. (2020). Catalytic properties of graphene oxide synthesized by a "Green" process for efficient abatement of Auramine-O cationic dye. *Analytical Chemistry Letters*, 10(1), pp. 21-32.
 12. Khataee, A., Rad, T. S., Nikzat, S., Hassani, A., Aslan, M. H., Kobya, M., & Demirbaş, E. (2019). Fabrication of NiFe layered double hydroxide/reduced graphene oxide (NiFe-LDH/rGO) nanocomposite with enhanced sonophotocatalytic activity for the degradation of moxifloxacin. *Chemical Engineering Journal*, 375, p. 122102.
 13. Khodadadi, B., Bordbar, M., & Nasrollahzadeh, M. (2017). Achillea millefolium L. extract mediated green synthesis of waste peach kernel shell supported silver nanoparticles: application of the nanoparticles for catalytic reduction of a variety of dyes in water. *Journal of colloid and interface science*, 493, pp. 85-93.
 14. Lin, F. H., & Doong, R. A. (2017). Catalytic nanoreactors of Au@ Fe₃O₄ yolk-shell nanostructures with various au sizes for efficient nitroarene reduction. *The Journal of Physical Chemistry C*, 121(14), pp. 7844-7853.
 15. Lumbaqué, E. C., Tiburtius, E. R. L., Barreto-Rodrigues, M., & Sirtori, C. (2019). Current trends in the use of zero-valent iron (Fe⁰) for degradation of pharmaceuticals present in different water matrices. *Trends in Environmental Analytical Chemistry*, 24, e00069.
 16. Pandey, P., Goel, V. K., Mishra, M., & Pandey, S. (2022). Comparative analysis of conventional X-ray chest Vs. NCCT chest in patients of blunt trauma chest: An observational study. *International Journal of Health Sciences*, 6(S5), 10179–10187. <https://doi.org/10.53730/ijhs.v6nS5.10763>
 17. Qasim, S., Zafar, A., Saif, M. S., Ali, Z., Nazar, M., Waqas, M., ... & Hasan, M. (2020). Green synthesis of iron oxide nanorods using Withania coagulans extract improved photocatalytic degradation and antimicrobial activity. *Journal of Photochemistry and Photobiology B: Biology*, 204, p. 111784.
 18. Roy, F., Taouil, A. E., Lallemand, F., Heintz, O., Moutarlier, V., & Hihn, J. Y. (2018). Alkanethiol self-assembling on gold: Influence of high frequency ultrasound on adsorption kinetics and electrochemical blocking. *Ultrasonics sonochemistry*, 40, pp. 9-16.
 19. Samuel, M. S., Jose, S., Selvarajan, E., Mathimani, T., & Pugazhendhi, A. (2020). Biosynthesized silver nanoparticles using *Bacillus amyloliquefaciens*; Application for cytotoxicity effect on A549 cell line and photocatalytic degradation of p-nitrophenol. *Journal of Photochemistry and Photobiology B: Biology*, 202, p. 111642.
 20. Suandayani, N. K. T. ., Sutapa, G. N. ., & Kasmawan, I. G. A. . (2020). Quality control of X-rays with collimator and the beam alignment test tool. *International Journal of Physical Sciences and Engineering*, 4(3), 7–15. <https://doi.org/10.29332/ijpse.v4n3.468>
 21. Thamilselvan, A., Manivel, P., Rajagopal, V., Nesakumar, N., & Suryanarayanan, V. (2019). Improved electrocatalytic activity of Au@ Fe₃O₄ magnetic nanoparticles for sensitive dopamine detection. *Colloids and Surfaces B: Biointerfaces*, 180, pp. 1-8.

22. Thari, F. Z., Tachallait, H., El Alaoui, N. E., Talha, A., Arshad, S., Álvarez, E., ... & Bougrin, K. (2020). Ultrasound-assisted one-pot green synthesis of new N-substituted-5-arylidene-thiazolidine-2, 4-dione-isoxazoline derivatives using NaCl/Oxone/Na₃PO₄ in aqueous media. *Ultrasonics sonochemistry*, 68,p. 105222.
23. Vickers, N. J. (2017). Animal communication: when i'm calling you, will you answer too?. *Current biology*, 27(14), pp.713-715.
24. Vickers, N. J. (2017). Animal communication: when i'm calling you, will you answer too?. *Current biology*, 27(14),pp. 713-715.
25. Vijilvani, C., Bindhu, M. R., Frincy, F. C., AlSalhi, M. S., Sabitha, S., Saravanakumar, K., ... & Atif, M. (2020). Antimicrobial and catalytic activities of biosynthesized gold, silver and palladium nanoparticles from Solanum nigurum leaves. *Journal of Photochemistry and Photobiology B: Biology*, 202,p. 111713.
26. Widana, I.K., Sumetri, N.W., Sutapa, I.K., Suryasa, W. (2021). Anthropometric measures for better cardiovascular and musculoskeletal health. *Computer Applications in Engineering Education*, 29(3), 550-561. <https://doi.org/10.1002/cae.22202>